© 2020. Published by The Company of Biologists Ltd | Journal of Experimental Biology (2020) 223, jeb230763. doi:10.1242/jeb.230763

RETRACTION

Retraction: Whale jaw joint is a shock absorber

Alexander J. Werth and Haruka Ito

The authors are retracting *Journal of Experimental Biology* (2020) **223**, jeb211904 (doi:10.1242/jeb.211904).

The authors no longer have full confidence in their results because of inconsistencies in data collection. Technical issues led to unreliable data recording, which then led to erroneous calculations that affected the results published in the paper.

As the paper was featured in the Inside JEB section, the associated Inside JEB article has also been retracted (doi:10.1242/jeb.230771).

The authors apologise to readers for any inconvenience caused.

© 2020. Published by The Company of Biologists Ltd | Journal of Experimental Biology (2020) 223, jeb211904. doi:10.1242/jeb.211904

SHORT COMMUNICATION

Whale jaw joint is a shock absorber

Alexander J. Werth[1,*] and Haruka Ito[2]

ABSTRACT

The non-synovial temporomandibular jaw joint of rorqual whales is presumed to withstand intense stresses when huge volumes of water are engulfed during lunge feeding. Examination and manipulation of temporomandibular joints (TMJs) in fresh carcasses, plus CT scans and field/lab mechanical testing of excised tissue blocks, reveals that the TMJ's fibrocartilage pad fully and quickly rebounds after shrinking by 68–88% in compression (by axis) and stretching 176–230%. It is more extensible along the mediolateral axis and less extensible dorsoventrally, but mostly isotropic, with collagen and elastin fibers running in all directions. The rorqual TMJ pad compresses as gape increases. Its stiffness is hypothesized to damp acceleration, whereas its elasticity is hypothesized to absorb shock during engulfment, allow for rotation or other jaw motion during gape opening/closure, and aid in returning jaws to their closed position during filtration via elastic recoil with conversion of stored potential energy into kinetic energy.

KEY WORDS: Cetacea, Mysticete, Temporomandibular, TMJ, Morphology, Biomechanics, Elasticity

INTRODUCTION

Rorquals (groove-throated whales, Balaenopteridae) include humpback, fin and blue whales, the largest animals that have ever lived. During ram-propelled lunge feeding on schooling fish and zooplankton, the jaws open wide to engulf massive volumes of prey-laden water, >70 m^3 in blue whales (*Balaenoptera musculus*; Goldbogen et al., 2012) and 30–40 m^3 in humpbacks (*Megaptera novaeangliae*; Simon et al., 2012). Even in the smallest rorqual species, northern and Antarctic minke whales (*Balaenoptera acutorostrata*, *Balaenoptera bonaerensis*), the engulfed water volume can be conservatively estimated at 3–6 m^3 based on scaling of oral and total body size (Werth et al., 2018a). By powering whales' forward locomotion, the flukes and tail stock musculature develop the power necessary for lunge feeding (Goldbogen et al., 2017), but the mandibles and temporomandibular joint (TMJ) presumably bear the brunt of the enormous drag forces generated when gape opens to accommodate water filling the greatly expanded oral pouch. Although no bite forces are encountered and the TMJ lies at the fulcrum of jaw movement, these mandibular and TMJ stresses likely pose a formidable challenge.

Whereas bowhead and right whales (Balaenidae) possess a typically mammalian mid-fixed synovial TMJ (Beauregard, 1882; Lambertsen et al., 1989), the rorqual TMJ has a large fibrocartilage pad but no joint capsule, synovial membrane or discrete articulating disc of hyaline cartilage (Brodie, 2001; Bouetel, 2005). The temporal glenoid cavity and head of the mandibular condyle are covered with smooth hyaline cartilage, but there is no cartilage between the fibrocartilage pad and the skull's mandibular fossa (Werth and Ito, 2017). The gray whale's (Eschrichtiidae) intermediate TMJ has a ventral joint cavity yet also a rudimentary fibrocartilage pad (El Adli and Perrin, 2015). Rorqual TMJ anatomy has long attracted attention (Carte and MacAlister, 1868; Beauregard, 1882; Benham, 1882; Schulte, 1916) but no functional investigation has been published to date.

However, several studies (Brodie, 1977; Pivorunas, 1977; Lambertsen, 1983; Lambertsen et al., 1995; Potvin et al., 2010; Goldbogen et al., 2017) concluded that the rorqual TMJ withstands intense forces as jaws are fully abducted during engulfment and to keep jaws closed (adducted) during rapid swimming. Further research has documented remarkable biomechanical properties, especially extreme elasticity or flexibility, of various rorqual oral tissues related to lunge feeding, including the ventral groove blubber or VGB (Orton and Brodie, 1987; Shadwick et al., 2013), nerves (Pyenson et al., 2015; Vogl et al., 2015; Lillie et al., 2017), blood vessels (Gosline and Shadwick, 1996; Lillie et al., 2013), sublingual fascia (Werth et al., 2019) and baleen (Werth et al., 2018b). This study focuses on the biomechanical properties of the rorqual TMJ, in particular its response to compressive, tensile and shear stresses; histological study and investigation of joint motion are ongoing. We hypothesized, based on the irregular array of collagen and elastin fibers in the TMJ's fibrocartilage pad, that it might be mechanically anisotropic and show high levels of elasticity, particularly along specific orthogonal axes.

MATERIALS AND METHODS

We examined the TMJ of seven deceased minke whale specimens, including four *B. acutorostrata* Lacépède 1804 (two adult: female 6.02 m body length, NEAq.MH.87.586.Ba stranded normal/fresh Code 2 at Truro, MA, USA; and female 4.6 m, 06-030.18.786 stranded normal/fresh Code 2 at Corolla, NC, USA; one juvenile: female 3.4 m stranded normal/fresh Code 2 at Virginia Beach, VA, USA; and one fetal: female 1.46 m, NEAq.MH,88.Bxx.Ba, mother stranded normal/fresh Code 2 at Cape Cod, MA, USA), and three fetal *B. bonaerensis* Burmeister 1867 (all ICR JARPA: male 1.45 m 03/04 318F, male 2.05 m 03/04 402F, female 2.09 m 05/06 486F). We examined/tested TMJs of three fin whales, *Balaenoptera physalus* (Linnaeus 1758) (two adult: male 17.68 m 24.7.F14.054, female 20.46 m 24.7.H9.F14.055; and one fetal: female 3.25 m 24.7.H8.F14.048F; all normal/fresh Code 2 at Hvalfjörður, Iceland). We dissected three additional rorqual TMJs (one sei whale, *Balaenoptera borealis* Lesson 1828; two humpback, *Megaptera novaeangliae* Borowski 1781) and performed field biomechanical tests on one of the humpback whales.

All specimens were dissected according to applicable statutes; no tissues were imported. For load cycle testing, larger cube-shaped tissue samples 10 cm on each side (1000 cm^3) (Fig. 1) were excised from the left and right TMJ pad of each non-fetal northern minke whale, with a smaller cube 5 cm on each side (125 cm^3) excised

[1]Department of Biology, Hampden-Sydney College, Hampden-Sydney, VA 23943 USA. [2]National Research Institute of Fisheries Science, Japan Fisheries Research and Education Agency, Yokohama, Kanagawa 236-8648, Japan.

*Author for correspondence (awerth@hsc.edu)

A.J.W., 0000-0002-7777-478X

Received 5 August 2019; Accepted 26 February 2020

Journal of Experimental Biology (2020) 223, jeb211904. doi:10.1242/jeb.211904

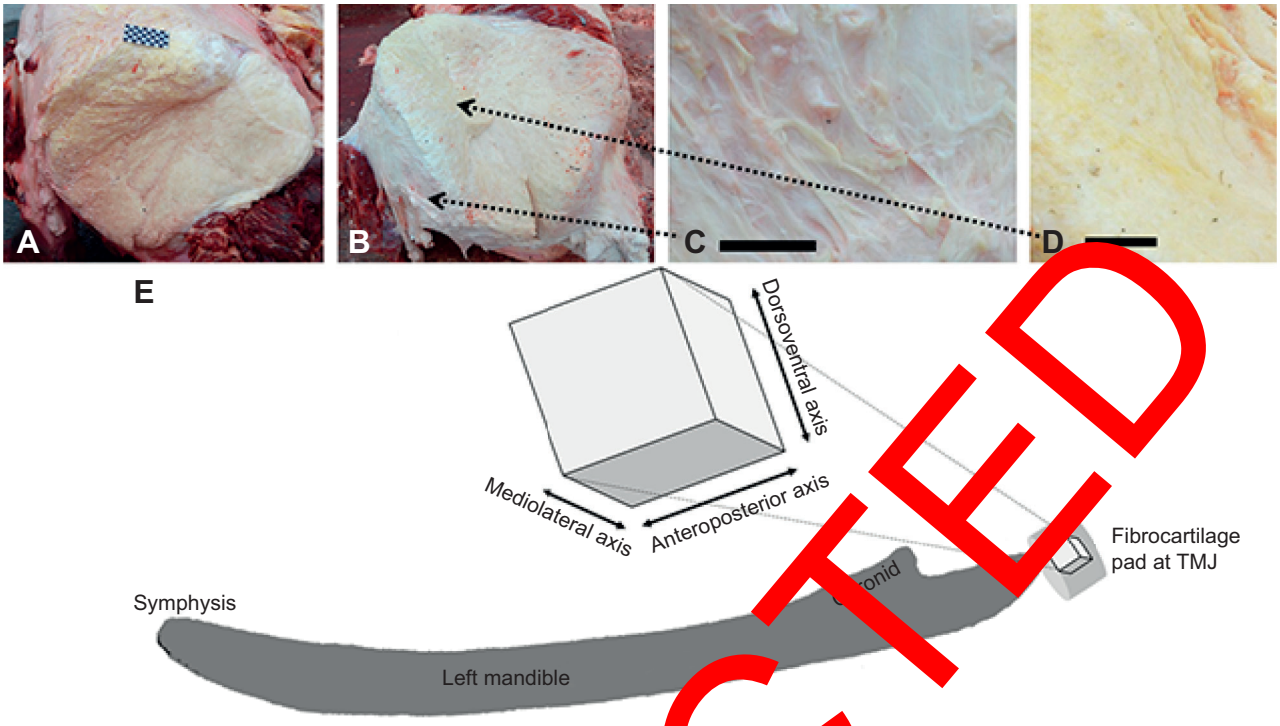

Fig. 1. The rorqual temporomandibular joint (TMJ). (A,B) The large fibrocartilage pad closely connects and adheres to the temporal bone (A) and mandibular condyle (B). A and B show the same bisected pad of a fin whale; the scale in A shows 1 cm squares. (C,D) Close-up views of white collagen and yellow elastin fibers within pad B. Scale bars: 1 cm. (E) Schematic view of the tissue blocks excised from the TMJ pad and the three axial dimensions for mechanical testing.

from the fetal northern minke whale's left TMJ. For initial strength (failure) testing, cube-shaped tissue blocks 5 cm on each side (125 cm^3) were excised from the left and right TMJ pads of the two adult northern minke whales, with smaller (64 cm^3) cubes removed from the fetal northern minke whale's left TMJ. This yielded a total of seven blocks (six adult/subadult, one fetal) for load to failure and nine blocks (six adult, three fetal) for non-destructive testing to failure points along perpendicular orthogonal axes. All blocks were removed from the fibrocartilage pad center, so that all six faces were of flat, sliced tissue. All blocks were cut with a large straight knife, with the TMJ pad removed from all bony attachments, placed on a stainless steel tray and pushed against a flat acrylic sheet so that straight cuts could be made with no or minimal need for later trimming in the lab. All excised tissue blocks were immediately frozen on site (−20°C) for transport and storage. Because samples had no landmarks or other features, care was taken to mark axial orientations with permanent ink as blocks were excised and handled. Samples were also taken for future histological analysis. Blocks were thawed at room temperature 1–30 months after collection, freezing for later testing of mechanical properties. The Antarctic minke whale specimens were scanned via CT imaging and dissected but not sampled for biomechanical testing. CT scans were conducted with a Siemens SOMATOM Spirit scanner (Munich, Germany) and analyzed with 3D medical imaging software (OsiriX MD 11.0 DICOM Viewer, Pixmeo, Geneva, Switzerland). The fin, humpback and sei whale TMJs were dissected and examined in the field, with field testing of compressive and tensile loading of one TMJ pad from each of the three fin whales and one of the humpback whales but not the sei whale, whose tissues were judged to be too deteriorated for proper biomechanical testing.

For laboratory material testing, thawed 125 cm^3 tissue blocks of the northern minke whales were initially tested for uniaxial strength in three orthogonal axes (dorsoventral, mediolateral and anteroposterior) following the ink markings for orientation. Tissue samples were loaded in compression or tension with a Mark-10 ES30 universal testing machine with M4-200 force gauge running MesurTMGauge recording software (Copiague, NY, USA). For compressive testing, samples were compressed between circular plates (Mark-10 G1009-2) affixed to the end of a mobile piston; for tensile testing, samples were clamped with wedge grips (Mark-10 G1061-3) with sharp 8 mm teeth that penetrated the tissue to hold it firmly in place. Sample cubes were not otherwise cut or punctured, and were tested to maximal compression and tension as judged by destruction (puncture or extrusion and tearing, respectively) of tissue fibers, with peak forces recorded in N and deformation in mm. Resulting deformation was recorded during loading/unloading cycles with the force gauge software as well as a data-linked Mitutoyo Digimatic micrometer (Kanagawa, Japan) to record tissue displacement (strain) due to applied tensing or compressing force.

Next, each of the seven larger (1000 cm^3 adult or 125 cm^3 fetal) tissue blocks was load tested uniaxially and sequentially in three dimensions (anteroposterior, dorsoventral and mediolateral, with N=20 loading/unloading cycles along each axis) to 95% of the same maximal compressive and tensile strengths determined during the earlier failure testing. As with the strength testing, both stress and strain were recorded with the MesurTMGauge software and strain was additionally recorded with a digital micrometer physically attached and data-linked to the testing machine. With N=20 loading/unloading cycles for all seven tissue blocks, the combined total was N=140 for compressive and N=140 for tensile tests along each of the three orthogonal axes. However, because the fetal tissue sample was smaller in size and came from a much younger (prenatal) animal, its results were not included in the pooled load cycle data (Fig. 2), which included N=360

Journal of Experimental Biology (2020) 223, jeb211904. doi:10.1242/jeb.211904

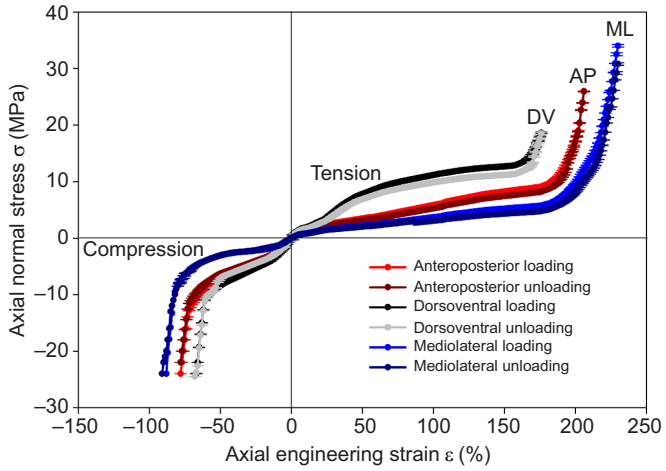

Fig. 2. Loading profile of the TMJ. Stress–strain curves combined for left and right TMJ pads from 3 adult/subadult northern minke whale specimens (6 pads total) for uniaxial testing in all 3 dimensions during loading (N=120 total tests along each axis) and unloading (N=120 total tests along each axis) (means±s.d.). The rorqual TMJ is highly elastic, especially in mediolateral compression/tension, and least elastic in dorsoventral compression/tension. AP, anteroposterior; DV, dorsoventral; ML, mediolateral.

compressive and N=360 tensile tests (20 per sample×6 samples×3 axes), so that N=720 total load cycles.

For the other species, TMJ fibrocartilage pads were dissected and examined in the field, with simpler biomechanical testing of fresh tissue blocks from fin and humpback whales. Samples of these species were not removed and frozen for lab testing. Whole M fibrocartilage pads and excised 10×10×10 cm blocks (1000 cm^3, equivalent to those from minke whales, and also cut with a la straight knife as pads were held flat against lucite she were teste in compression with a Mark-10 M4-200 force uge (piague) pushing tissue between flat plates, and in te ion with Pesola Macroline spring scale (Schindellegi, Switze nd) disp in N, again testing N=20 along each ortho onal maximal axial compressive and tensile strength was determin in these field tests, but the load cycling was perf ed to 95% of maximal (failure) compression and tensio as termined by the earlier testing on northern minke whal tissue sa les. Additional field studies employed either slow or rapidly app d forces precisely maintained at 50 N to de mine whether the TMJ pad material might be viscoelastic or i recovery herwise time limited such that it could aid in dam g accel tion or absorbing and storing energy. Field and lab (li im strength d load cycling) results were analyzed via t-tests determin whether data (e.g. from different speci ens, s and sp ies were statistically significant.

RESULTS AND DISC SION

In all speci s ex mined, the TMJ was a heterogeneous matrix of fibrocartilage i ding abundant white collagen and yellow elastin fibers (Fig. 1). Ho ver, no discernible differences in pad regions could be detected *in* s or in excised samples. There were scattered fibroblasts, adipocytes and regions of what appeared to be highly hydrated chondrocytes. The entire fibrocartilage pad was approximately 0.007 m^3 in volume in a 6 m minke whale (0.136 m^3 in a 20 m fin whale). The pad was flexible to the touch and easily deformed 10–15 cm: when pushed, pulled or subjected to shear (≤70 N), the tissue resumed its original form within 1.5±0.3 s (mean±s.d.). Manipulation of fresh carcasses showed flexible jaws cannot easily be misaligned or disarticulated unless tissues are cut. When manually opened, jaws tended to close on their own (within 4 s in minke whales), although this could be due to many factors or non-TMJ tissues. Mandibular rotation (medial roll and lateral yaw) accompanied abduction; the pad twisted but easily resumed its original form.

Strength testing of the minke whale tissue revealed maximal loading of 29 N in compression (mean±s.d. 29.2±0.2 N dorsoventral, 29.4±0.2 N anteroposterior, 29.5±0.3 N mediolateral, all N=8) and 22–40 N in tension (22.3±0.3 N dorsoventral, 29.6±0.3 N anteroposterior, 39.7±0.3 N mediolateral) ding profiles (Fig. 2) indicated a soft, highly elastic tissue upporti he hypothesized rorqual TMJ flexibility. When c pressed, eac block shrank 70–90% along any axis with a ication of 24–2 MPa. When pulled under tensile forces of 19–35 Pa, the block increased by 176–224% of their origina ze (Fig. 2 oadin and unloading curves were similar, rev ing little hystere g. 2). There was close agreement of for gauge a micrometer displacement data (P=0.92). Field tests i cated o signific t difference (P=0.81) between fresh TM issue immedi y postmortem or frozen and thawed fo ater labora testi g. This elasticity range is comparable t r whale oral tis noted above, and accords with field data fresh whale TMJ pads, which also demonstrated compressive strains o –80% (mean±s.d. 68.4±1.3%, N=48) and tensile ins of 120–16 (129.7±4.1%, N=48); data from the sin humpback TMJ pad showed even greater elasticity (mean±s.d. c pressive strai 73.2±3.4%, tensile strain 138.6±4.8%, N=25). S ecies difference etween TMJ pads of minke versus fin (P=0.32) a humpback (P= 56) whales were not significant. No differences wer und betw n sex or size/age class, except that the fetal minke whale ue was substantially more elastic than adult tissue =0.09), perhaps because mature collagen typically develops c s or from other age-related histological change.

Our results suggest the fibrocartilage pad's mechanical anisotropy is limited (Fig. 2), as stress/strain vary little between axes (P=0.51). The pad was least elastic in the dorsoventral plane, stretching 166% under tension (with mean±s.d. 18.6±0.13 MPa, N=120 for all trials) and −68% under compression (with 24.5±0.19 MPa). It was most elastic in the mediolateral plane, where it stretched 224% under tension (with 35.2±0.09 MPa) and −88% under compression (24±0.07 MPa). Stretching was intermediate in the anteroposterior plane, at 202% (with 26±0.21 MPa) in tension and −78% (with 24±0.17 MPa) in compression.

Preliminary histology results did not indicate obvious differences in axial fiber arrangement, yet suggested slightly more elastin fibers (perhaps 15–20% more) running anteroposteriorly and dorsoventrally. We presume the strong collagen fibers mainly resist tension and the yellow elastin fibers aid in recovery from tensile and compressive loading, as in typical fibrocartilage (Benjamin and Ralphs, 1998) as well as other heavily loaded cetacean tissues that show high stiffness and elasticity (Gosline and Shadwick, 1996; Shadwick, 1999). Despite its close proximity to the ear, the fibrocartilage pad is unlikely to play a role in sound transmission, although its acoustic properties should be analyzed.

How these triaxial stress/strain results relate to jaw movements is uncertain. However, dissected TMJs enabled us to observe fibrocartilage pad alteration during jaw manipulation. Further, CT scans (Fig. 3) yielded internal views showing osteological relationships and dimensions plus soft tissue deformation during jaw abduction/adduction. The pad is not a wholly constant-volume structure but its deformation largely follows a simple scheme. As gape increases from zero (mouth closed) to full (opened), the pad shortens overall but appears to become compressed mainly in its ventral portion, whereas its dorsal portion is tensed. At the same

Journal of Experimental Biology (2020) 223, jeb211904. doi:10.1242/jeb.211904

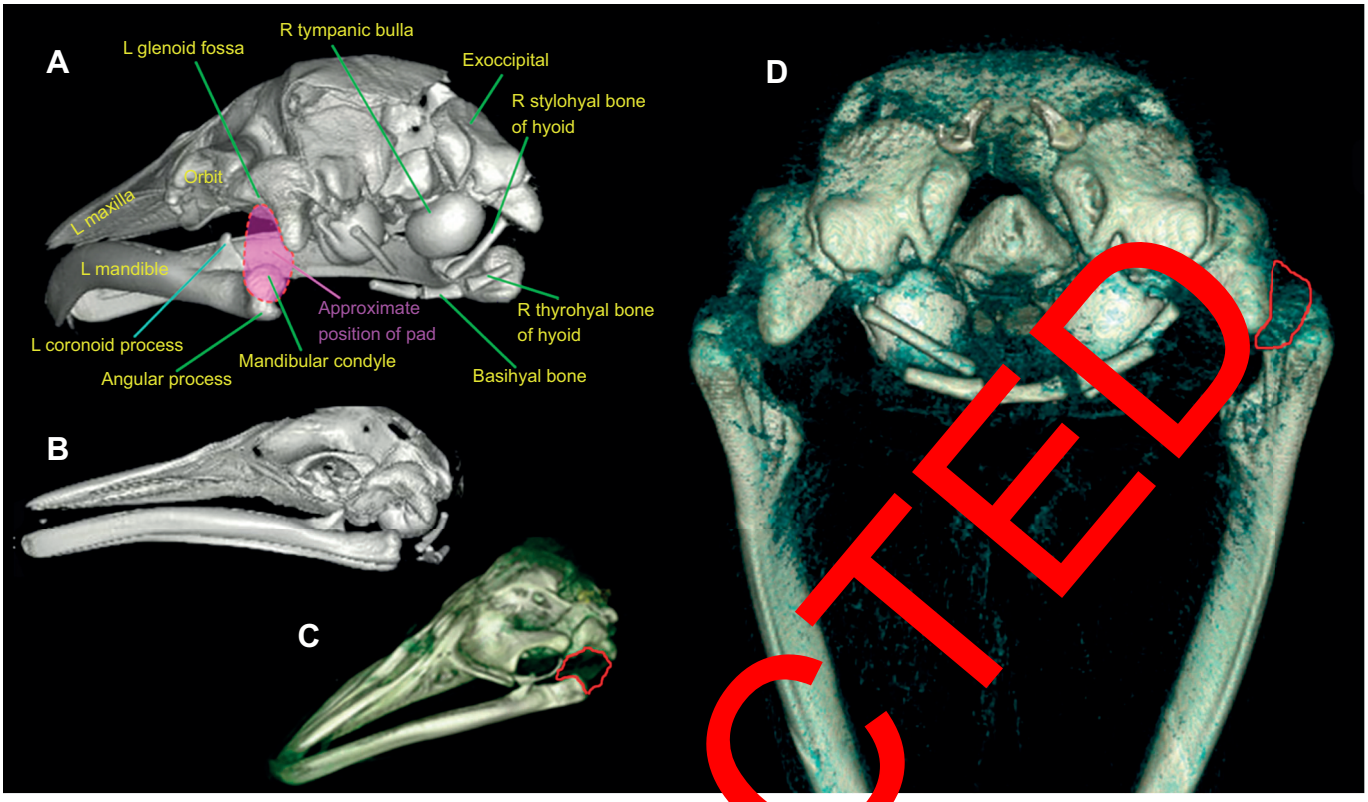

Fig. 3. CT scans of Antarctic minke whale head. (A) Posterolateral, (B) lateral, (C) dorsol[illegible] posterior (full gape) views show bony elements (cranium/mandibles/hyoid) and soft tissues including the TMJ pad [approximat[illegible]ched red oval in A and outlined in red in C (left pad) and D (right pad)]. With full gape (jaw abduction, D), the pad becomes compressed anteroposteriorly a[illegible]tly expanded mediolaterally.

time, the anteroposteriorly compressed pad extends mediolatera[illegible] (by about 40–60%) and to a lesser degree dorsoventr[illegible] (10–15%). Although uniaxial testing along individual axes yields interesting and potentially useful controlled data, [illegible] cannot replicate simultaneous loading along three axes, as a[illegible]ost certa[illegible] *in vivo*.

Our results, including equivocal re[illegible]ts of co[illegible]ssive/tensile tests conducted with varying spe[illegible] suggest the [illegible]ual TMJ fibrocartilage pad could act lik[illegible] an[illegible]icular shock-absorbing cushion whose stiffness damps a[illegible]celeration[illegible] viscous friction and deformable elasticity absorb[illegible] shock during p[illegible] engulfment. The pad could allow for mand[illegible]ular rotation and dis[illegible]cement during gape opening/closure to[illegible] eatly ex[illegible]nd buccal volume, and could aid in returning jaws t[illegible] closed [illegible]sition during filtration via elastic recoil with conversion o[illegible] re[illegible] otential e[illegible]gy into kinetic energy. The role during rapid lung[illegible] eeding [illegible] rorquals' capacious oral pouch and ela[illegible]c, a[illegible]rdion-l[illegible] th[illegible]t pleats (Pivorunas, 1977; Orton and B[illegible]die, 198[illegible]; Goldboge[illegible], 2010; Shadwick et al., 2013) depends o[illegible]he jaw jo[illegible]'[illegible]bility to open widely and to close against huge loadi[illegible] forc[illegible] generated by the massive volume of engulfed water and ens[illegible] drag (Lambertsen, 1983; Arnold et al., 2005; Potvin et al., 201[illegible] Previous studies (Lambertsen et al., 1995; Lambertsen and Hint[illegible]004; Arnold et al., 2005; Goldbogen et al., 2011) concluded that the fully adducted (closed) jaw forms some sort of oral seal which, when combined with other oral adaptations, enables rorquals to stabilize jaws and control gape opening/closure while potentially minimizing energetic costs. The loose, flexible TMJ and mandibular symphysis and consequent wide gape (Fitzgerald, 2012; Pyenson et al., 2012) may have fueled rorquals' trophic success and consequent adaptive radiation (Kimura, 2002; Thewissen, 2014; Marx et al., 2016; Goldbogen et al., 2019).

Acknowledgements
For field access we are grateful to Kristjan Loftsson and staff of Hvalur in Iceland, Dr Y. Fujise at the Institute of Cetacean Research in Japan, and Erin Fougeres, Bill McLellan and participants/organizers of the NOAA/NMFS Marine Mammal Stranding Network of USA. For ideas and assistance, we thank colleagues including Bob Shadwick, Jeremy Goldbogen, Nick Pyenson, Jean Potvin, Margo Lillie, Wayne Vogl, Tom Ford, Pierre-Henry Fontaine, Keiichi Ueda, Seiji Otani, Tatsuya Isoda, Hiroshi Sawamura and Hiroto Ichishima.

Competing interests
The authors declare no competing or financial interests.

Author contributions
Conceptualization: A.J.W., H.I.; Methodology: A.J.W., H.I.; Validation: A.J.W., H.I.; Formal analysis: A.J.W., H.I.; Investigation: A.J.W., H.I.; Resources: A.J.W., H.I.; Data curation: A.J.W.; Writing - original draft: A.J.W.; Writing - review & editing: A.J.W., H.I.; Visualization: A.J.W., H.I.; Supervision: A.J.W.; Project administration: A.J.W., H.I.

Funding
A.J.W. was funded by Hampden-Sydney College faculty grants and Trinkle research funds.

References

Arnold, P. W., Birtles, R. A., Sobtzick, S., Matthews, M. and Dunstan, A. (2005). Gulping behaviour in rorqual whales: underwater observations and functional interpretation. *Mem. Queensland Mus.* **51**, 309-332.
Beauregard, H. (1882). L'articulation temporomaxillaire chez les Cetaces. *J. d l'Anat. et la Physiol.* **18**, 16-26.
Beneden, P. J. (1882). Sur l'articulation temporomaxillaire chez les Cetaces. *Arch. de Biol.* **3**, 669-673.
Benjamin, M. and Ralphs, J. R. (1998). Fibrocartilage in tendons and ligaments: an adaptation to compressive load. *J. Anat.* **193**, 481-494. doi:10.1046/j.1469-7580.1998.19340481.x
Bouetel, V. (2005). Phylogenetic implications of skull structure and feeding behavior in balaenopterids (Cetacea, Mysticeti). *J. Mamm.* **86**, 139-146. doi:10.1644/1545-1542(2005)086<0139:PIOSSA>2.0.CO;2

Brodie, P. F. (1977). Form, function, and energetics of Cetacea: a discussion. In *Functional Anatomy of Marine Mammals* (ed. R. J. Harrison), pp. 45-58. New York: Academic Press.
Brodie, P. F. (2001). Feeding mechanics of rorquals *Balaenoptera* sp. In *Secondary Adaptations of Tetrapods to Life in Water* (ed. J. M. Mazin and V. de Buffrénil), pp. 345-352. Munich: Verlag.
Carte, A. M. and Macalister, A. (1868). On the anatomy of *Balaenoptera rostrata*. *Phil. Trans. Roy. Soc. Lond.* **185**, 201-261. doi:10.1098/rstl.1868.0009
El Adli, J. J. and Deméré, T. A. (2015). On the anatomy of the temporomandibular joint and the muscles that act upon it: observations on the gray whale, *Eschrichtius robustus*. *Anat. Rec.* **298**, 680-690. doi:10.1002/ar.23109
Fitzgerald, E. M. G. (2012). Archaeocete-like jaws in a baleen whale. *Biol. Lett.* **8**, 94-96. doi:10.1098/rsbl.2011.0690
Goldbogen, J. A. (2010). The ultimate mouthful: lunge feeding in rorqual whales. *Am. Sci.* **98**, 124-131. doi:10.1511/2010.83.124
Goldbogen, J. A., Calambokidis, J., Oleson, E., Pyenson, N. D., Schorr, G. and Shadwick, R. E. (2011). Mechanics, hydrodynamics and energetics of blue whale lunge feeding: efficiency dependence on krill density. *J. Exp. Biol.* **214**, 131-146. doi:10.1242/jeb.048157
Goldbogen, J. A., Calambokidis, J., Croll, D. A., McKenna, M. F., Oleson, E., Potvin, J., Pyenson, N. D., Schorr, G., Shadwick, R. E. and Tershy, B. R. (2012). Scaling of lunge-feeding performance in rorqual whales: mass-specific energy expenditure increases with body size and progressively limits diving capacity. *Func. Ecol.* **26**, 216-226. doi:10.1111/j.1365-2435.2011.01905.x
Goldbogen, J. A., Cade, D. E., Calambokidis, J., Friedlaender, A. S., Potvin, J., Segre, P. S. and Werth, A. J. (2017). How baleen whales feed: the biomechanics of engulfment and filtration. *Ann. Rev. Mar. Sci.* **9**, 367-386. doi:10.1146/annurev-marine-122414-033905
Goldbogen, J. A., Cade, D. E., Wisniewska, D. M., Potvin, J., Segre, P. S., Savoca, M. S., Hazen, E. L., Czapanskiy, M. F., Kahane-Rapport, S. R., DeRuiters, S. K. et al. (2019). Why whales are big but not bigger: physiological drivers and ecological limits in the age of ocean giants. *Science* **366**, 1367-1372. doi:10.1126/science.aax9044
Gosline, J. and Shadwick, R. E. (1996). The mechanical properties of fin whale arteries are explained by novel connective tissue designs. *J. Exp. Biol.* **199**, 985-987.
Kimura, T. (2002). Feeding strategy of an early Miocene cetothere from the Toyama and Akeyo Formations, central Japan. *Paleontol. Res.* **6**, 179-189.
Lambertsen, R. L. (1983). Internal mechanism of rorqual feeding. *J. Mam.* **64**, 76-88. doi:10.2307/1380752
Lambertsen, R. H. and Hintz, R. J. (2004). Maxillomandibular cam articulation discovered in north Atlantic minke whale. *J. Mamm.* **85**, 446-452. doi:10.16[illegible] BRB-125
Lambertsen, R. H., Hintz, R. J., Lancaster, W. C., Hirons, A[illegible]reiton, [illegible] J., Moor, C. (1989). Characterization of the functional morphology of the mouth of the bowhead whale, Balaena mysticetus, with special emphasis on the [illegible] and filtration mechanisms. Report to the Department of Wi[illegible] Mana[illegible]ent. Barrow, Alaska: North Slope Borough.
Lambertsen, R. L., Ulrich, N. and Straley, J. (1995). Front[illegible]ndibular stay of Balaenopteridae: a mechanism for mo[illegible]tum recapture [illegible]ing feeding. *J. Mamm.* **76**, 877-899. doi:10.2307/138[illegible]
Lillie, M. A., Piscitelli, M. A., Vogl, A. W., Gosline, J. M. and Shadwick, R. E. (2013). Cardiovascular design in fin whales: high-stiffness arteries protect against adverse pressure gradients at depth. *J. Exp. Biol.* **216**, 2548-2563. doi:10.1242/jeb.081802
Lillie, M. A., Vogl, A. W., Gil, K. N. and Shadwick, R. E. (2017). Two levels of waviness are necessary to package the highly extensible nerves in rorqual whales. *Curr. Biol.* **27**, 673-679. doi:10.1016/j.cub.2017.01.007
Marx, F. G., Lambert, O. and Uhen, M. (2016). *Cetacean Paleobiology*. London: Wiley-Blackwell.
Orton, L. S. and Brodie, P. F. (1987). Engulfing mechanics of fin whales. *Can. J. Zool.* **65**, 2898-2907. doi:10.1139/z87-440
Pivorunas, A. (1977). The fibrocartilage skele[illegible]ted structures of the ventral pouch of balaenopterid whales. *J. M[illegible]n.* **151**, 299-[illegible] doi:10.1002/jmor.1051510207
Potvin, J., Goldbogen, J. A. and Shadw[illegible]R. E. (2010). Scalin[illegible]f lunge feeding in rorqual whales: an integrated model of e[illegible]ment duration. *J. Theor. Biol.* **267**, 437-453. doi:10.1016/j.jtbi.2010.0[illegible]26
Pyenson, N. D., Goldbogen, J. A., Vogl, A. W., S[illegible]mary, [illegible], Drake, R. L. and Shadwick, R. E. (2012). Di[illegible]very of a sensory o[illegible]at coordinates lunge feeding in rorqual whales. *Nat.* **485**, 49[illegible]01. doi:10.10[illegible]/nature11135
Shadwick, R. E. (1999). [illegible]echanical [illegible]esign in arteries. *J. Exp. Biol.* **202**, 3305-3313.
Shadwick, R. E., Go[illegible]ogen, J. [illegible]Potvin, J., [illegible]enson, N. D. and Vogl, A. W. (2013). Novel m[illegible]e and connecti[illegible]ssue d[illegible]gn enables high extensibility and controls engul[illegible]t volume in lunge-[illegible]g rorqual whales. *J. Exp. Biol.* **216**, 2691-2701. doi:10.[illegible]/jeb.081752
Schulte, H. (1916). A[illegible]my of a foetus of *Balaenoptera borealis*. Monographs of Pacific Cetacea. *Mem. Am[illegible]us. Nat. Hist.* **1**, 389-502.
Simon, M., Johnson, M. and [illegible]dsen, P. T. (2012). Keeping momentum with a m[illegible]ful of water: behavior and kinematics of humpback whale lunge feeding. *J. Exp. Biol.* **215**, 3786-3798. doi:10.1242/jeb.071092
Tw[illegible]wissen, J. G. M. (2014). *The Walking Whales*. Berkeley: Univ. of California Press.
V[illegible] A. W., Lillie, M. [illegible] Piscitelli, M. S., Goldbogen, J. A., Pyenson, N. D. and S[illegible]dwick, R. E. (2[illegible]5). Stretchy nerves: essential components of an extreme feed[illegible]echan[illegible]in rorqual whales. *Curr. Biol.* **25**, 360-361. doi:10.1016/j.cub.2015.03.0[illegible]
Werth, A. J. and Ito, H. (2017). Sling, scoop, and squirter: anatomical features [illegible]prey transport, processing, and swallowing in rorqual whales (Mammalia: Mysticeti). *Anat. Rec.* **300**, 2070-2086. doi:10.1002/ar.23606
Werth, A. J., Lillie, M. A., Piscitelli, M. S., Vogl, A. W. and Shadwick, R. E. (2019). Slick, stretchy fascia underlies the sliding tongue of rorquals. *Anat. Rec.* **302**, 735-744. doi:10.1002/ar.24035
Werth, A. J., Potvin, J., Shadwick, R. E., Jensen, M. M., Cade, D. E. and Goldbogen, J. A. (2018a). Filtration area scaling and evolution in mysticetes: trophic niche partitioning and the curious cases of sei and pygmy right whales. *Biol. J. Linn. Soc.* **125**, 264-279. doi:10.1093/biolinnean/bly121
Werth, A. J., Rita, D., Rosario, M. V., Moore, M. J. and Sformo, T. L. (2018b). How do baleen whales stow their filter? A comparative biomechanical analysis of baleen bending. *J. Exp. Biol.* **221**, 1-9. doi:10.1242/jeb.189233